

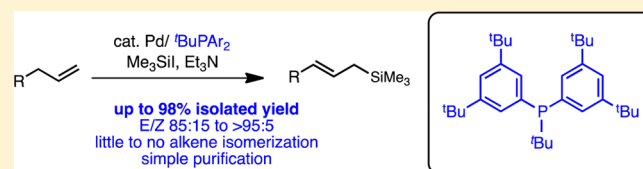
## Rational Design of a Second Generation Catalyst for Preparation of Allylsilanes Using the Silyl-Heck Reaction

Jesse R. McAtee, Glenn P. A. Yap, and Donald A. Watson\*

Department of Chemistry and Biochemistry, University of Delaware, Newark, Delaware 19716, United States

### Supporting Information

**ABSTRACT:** Using rational ligand design, we have developed of a second-generation ligand, bis(3,5-di-*tert*-butylphenyl) (*tert*-butyl)phosphine, for the preparation of allylsilanes using the palladium-catalyzed silyl-Heck reaction. This new ligand provides nearly complete suppression of starting material alkene isomerization that was observed with our first-generation catalyst, providing vastly improved yields of allylsilanes from simple alkene starting materials. The studies quantifying the electronic and steric properties of the new ligand are described. Finally, we report an X-ray crystal structure of a palladium complex resulting from the oxidative addition of  $\text{Me}_3\text{SiI}$  using an analogous ligand that provides significant insight into the nature of the catalytic system.



## 1. INTRODUCTION

Allylsilanes are versatile nucleophiles in organic synthesis that possess numerous favorable properties, including low toxicity and high functional group compatibility.<sup>1</sup> We recently described a novel synthesis of allyl- (and vinyl-) silanes by palladium-catalyzed silylation of terminal alkenes using  $\text{Me}_3\text{SiI}$ .<sup>2–5</sup> This silyl-Heck reaction provides an expedient entry into these important nucleophiles using widely available alkene starting materials.<sup>6</sup> Although our initial conditions provided allylsilanes with good to excellent selectivities for the *trans* isomers and were functional-group tolerant, the yields of these reactions were moderate (typically ~60%) due to competitive isomerization of the alkene starting material.<sup>2</sup>

Guided by rational ligand design, we have sought improved catalysts that minimize competitive alkene isomerization and increase the yield of the allylsilane. We now report a second-generation ligand for the palladium-catalyzed silyl-Heck reaction that converts a broad range of terminal alkenes into allylsilanes with dramatically improved yields. In addition, these studies have deepened our understanding of the product-determining step that leads to allylsilane formation. Quantitative studies of the steric and electronic properties of the various ligands investigated, as well as stoichiometric experiments, provide insight into the palladium species involved in the oxidative addition of  $\text{Me}_3\text{Si—I}$ . These studies culminated in isolation and characterization of the first monomeric palladium complex from the oxidative addition of a silicon–halogen bond. In total, these studies have not only greatly improved the synthetic utility of the silyl-Heck reaction in the preparation of allylsilanes, but also significantly increased our understanding of the process.

## 2. RESULTS AND DISCUSSION

**2.1. Ligand Design Considerations.** In our previous study, we identified  $\text{tBuPPH}_2$  as an effective ligand for silyl-Heck

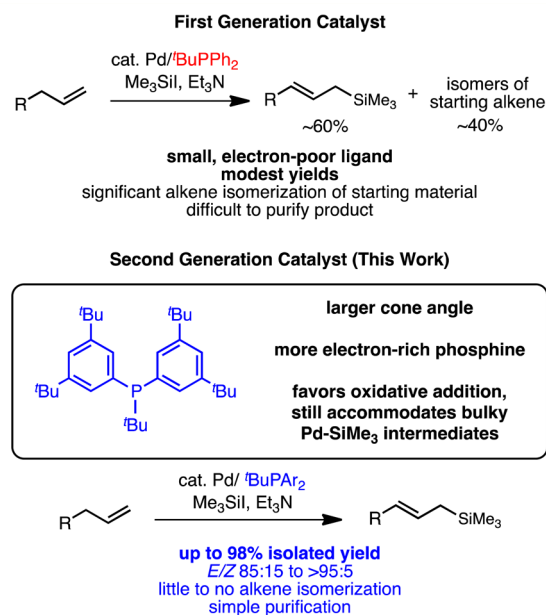


**Figure 1.** Rational design of 2nd generation catalyst for the silyl-Heck reaction.

reactions. This ligand was vastly superior to both all-aryl phosphines, such as  $\text{Ph}_3\text{P}$ , as well as all-alkyl phosphines, such as  $\text{Cy}_3\text{P}$  and  $\text{tBu}_3\text{P}$ .<sup>2</sup> We rationalized that the effectiveness of  $\text{tBuPPH}_2$  was due to it being sufficiently electron-rich to favor oxidative addition of the  $\text{Me}_3\text{Si—I}$  bond (in contrast to  $\text{Ph}_3\text{P}$ ), while being able to accommodate the large silyl group in the  $\text{Pd—SiMe}_3$  intermediates involved in the reaction (by rotation of the flat phenyl groups, in contrast to  $\text{Cy}_3\text{P}$  and  $\text{tBu}_3\text{P}$ ).

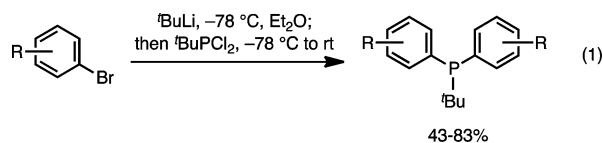
Received: May 30, 2014

Published: July 8, 2014

We recognized, however, that while the inclusion of phenyl groups might be necessary for steric reasons, the inductive electron-withdrawing nature of these aromatic substituents dramatically lowers the electron-density of the ligand compared to all-alkyl congeners (e.g.,  $\text{Cy}_3\text{P}$  and  ${}^t\text{Bu}_3\text{P}$ ). In addition,  ${}^t\text{BuPPh}_2$  is only a moderately sterically demanding ligand.

Large, highly electron-rich ligands have been shown to promote oxidative addition.<sup>7</sup> As it was likely that competition between oxidative addition to the Si—I bond (leading to productive silyl-Heck products) and background isomerization of the alkene starting material (likely by trace metal hydride species) was responsible for the limited yields of allylsilanes in our original report, we hypothesized that catalysts employing larger and more electron-rich phosphine ligands would further improve the reaction. Specifically, we hoped that by increasing the electron-donating character of the arene groups on the ligand backbone, a more efficient catalyst might arise. At the same time, additional substituents on the aromatic groups would increase the size of the ligand, potentially leading to further improvements in the reaction.

**2.2. Ligand Synthesis.** To investigate the possibility that larger, more electron-rich ligands would lead to more efficient allylsilane synthesis, we prepared a series of diaryl-*tert*-butyl phosphine ligands with varied electronic and steric properties of the aryl groups. These ligands were prepared by addition of the aromatic organolithium reagent to dichloro-*tert*-butylphosphine (eq 1). Yields ranged from 47 to 83% after purification by



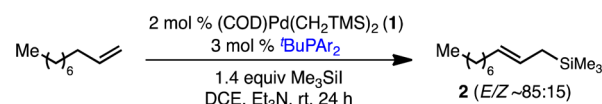
distillation or recrystallization. Further details regarding ligand synthesis are provided in the Supporting Information (SI).

**2.3. Ligand Optimization Studies.** To assess the effect of ligand design on the silyl-Heck reaction, we selected the coupling of 1-decene and  $\text{Me}_3\text{SiI}$  as our model system (Table 1). Our initial investigation compared the use of  ${}^t\text{BuPPh}_2$  (**3**) and  ${}^t\text{BuP}(4\text{-C}_6\text{H}_4\text{OMe})_2$  (**6**) as ligands under palladium-catalyzed conditions. Consistent with our hypothesis, the reaction involving the more electron-rich ligand **6** provided markedly higher yield of desired product **2** compared to that using  ${}^t\text{BuPPh}_2$  (entries 1 vs 4). Further, when ligands bearing meta electron-withdrawing substituents were employed (**4** and **5**, entries 2 and 3), lower yields were observed.

To further increase the electron-donor ability of the ligand, as well as its size, *para*-anisole derivatives bearing meta alkyl groups were prepared (ligands **7** and **8**, entries 5 and 6). The yield of desired product **2** improved with both methyl and *tert*-butyl substituents, and increased with the size of the alkyl group. With 3,5-di-*tert*-butyl-4-methoxyphenyl-derived ligand **8**, the product was produced in 92% yield.

For comparison, we also prepared the ligand series bearing *para*-dimethylamino substitution (ligands **9–11**). In this series, the results were less straightforward. The reaction involving ligand **9**, which lacked meta substitution, provided similar yields of **2** compared to  ${}^t\text{BuPPh}_2$  (entry 7). In contrast, the ligand bearing *meta*-methyl groups (**10**) provided increased yields (entry 8), similar to dimethylanisole ligand **7**. Surprisingly, however, the 3,5-di-*iso*-propyl-4-dimethylaminophenyl derived **11** provided vastly superior results, giving the desired product in nearly quantitative yield (entry 9).

**Table 1. Optimization of Conditions Through Rational Ligand Design**



Entry	Ligand	Ar	R	Yield <sup>a</sup>
1	<b>3</b>		H	60%
2	<b>4</b>		OMe	55%
3	<b>5</b>		CF <sub>3</sub>	0%
4	<b>6</b>		H	74%
5	<b>7</b>		Me	85%
6	<b>8</b>		<i>t</i> Bu	92%
7	<b>9</b>		H	61%
8	<b>10</b>		Me	87%
9	<b>11</b>		<i>i</i> Pr	99%
10	<b>12</b>		Me	75%
11	<b>13</b>		<i>i</i> Pr	82%
12	<b>14</b>		<i>t</i> Bu	99%

<sup>a</sup>Yield determined by NMR using internal standard (1,3,5- $\text{C}_6\text{H}_3(\text{OMe})_3$ ). Yield reflects total silylated products (allylsilane + trace vinyl silane); in all cases, allylsilane/vinylsilane  $\geq$  93:7, *E*-allyl/*Z*-allyl  $\approx$  85:15.

While highly encouraging, this latter result was also perplexing. Examination of molecular models revealed that the flanking isopropyl groups force the dimethylamino group into a conformation where the nonbonding electron pair of the nitrogen is perpendicular to the  $\pi$ -system of the aromatic ring (Figure 2). In such a conformation, little electronic benefit from

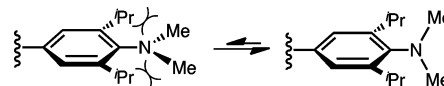
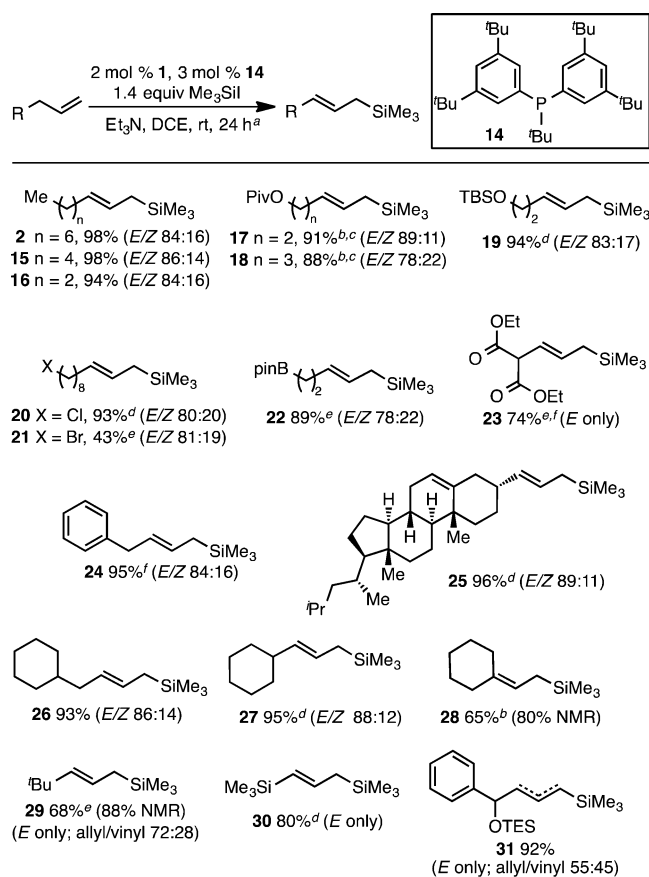


**Figure 2.** Conformational analysis of dimethylamino group in ligand **11**.

the dimethyl amino group is expected. This analysis led us to question the need for a *para*-heteroatom substituent.

Accordingly, we prepared one final series of ligands bearing only *meta*-alkyl substituents on the aromatic rings (ligands **12–14**). Pleasantly, and surprisingly, this series of ligands was also highly effective in the model transformation. Ligands bearing either methyl or isopropyl groups showed significant improvement over  ${}^t\text{BuPPh}_2$  (entries 10 and 11). Most significantly, however, the ligand bearing *meta,meta*-di-*tert*-butylphenyl groups (**14**) provided product **2** in 99% assay yield (entry 12). As ligand **14** can be easily prepared on multigram scale in only a single step from commercially available materials and is air stable (no detectable oxidation was observed by <sup>31</sup>P NMR after one year of storage on the benchtop under air), we selected this ligand to explore as a second generation ligand for the preparation of allylsilanes.

**2.4. Substrate Scope of Allylsilane Synthesis Using Ligand 14.** Using ligand **14**, vastly improved yields of allylsilanes are obtained with a broad range of  $\alpha$ -olefin substrates (Figure 3). In general, high yields, good *E/Z* selectivities, and outstanding allyl/vinyl selectivities were observed.<sup>8</sup> For example, the model substrate gave rise to allylsilane **2** in 98% isolated yield as a 84:16 mixture of *E/Z* isomers, with only trace amounts ( $\leq$ 7%) of the



<sup>a</sup> Unless otherwise noted, contains  $\leq 10\%$  *E*-vinylsilane. <sup>b</sup> Using 8 mol % **1** and 12 mol % **14**. <sup>c</sup> Contains 12% *E*-vinylsilane. <sup>d</sup> Using 4 mol % **1** and 6 mol % **14**. <sup>e</sup> Using 10 mol % **1** and 10 mol % **14**. <sup>f</sup> Contains 8–11% homoallylsilane.

**Figure 3.** Scope of silyl-Heck reaction to form allylsilanes with second-generation ligand.

vinylsilane isomer. Similar results were obtained for other *n*-alkyl  $\alpha$ -olefins (e.g., **15** and **16**). The allyl vs vinyl and *E*-allyl vs *Z*-allyl selectivity are very similar to the first-generation catalyst system.<sup>2</sup> Importantly, however, and in contrast to the earlier system using <sup>t</sup>BuPPh<sub>2</sub>, almost no alkene isomerization of the starting material was observed. This not only significantly improves the yield of the allylsilane, but also greatly simplifies purification of the product.

The silyl-Heck reaction also demonstrates a broad range of functional group compatibility, although in some cases slightly greater catalyst loadings were required to achieve high yields (see Figure 3). Protected alcohols, including pivaloyl esters and silyl ethers can be used without incident (**17**–**19**). Alkyl halides are also well tolerated. With alkyl chlorides, high yields of the desired allylsilane are achieved (**20**). Alkyl bromides can also be used, but higher catalyst loading and a modified metal to ligand ratio (1:1) are required to obtain desired product **21** in modest yield. Alkyl boronic esters participate smoothly in this reaction giving a potentially versatile dimetalloid (**22**).

Malonates are tolerated in the reaction, as shown by **23**. In this particular case, a small amount of alkene isomerization (11%) was observed, wherein the alkene moved into conjugation with the diester group, giving the homoallylsilane. A similar result was obtained with the use of homoallylbenzene. In this case, product **24** was contaminated with approximately 8% of the *E*-homoallylsilane, wherein the alkene moved into conjugation with the phenyl group. We believe that the fact that such a low

amount of alkene isomers are observed, even in these highly thermodynamically favorable cases, suggests that the observed allylsilanes are the kinetic products of the silyl-Heck reaction and are not the result of postreaction alkene isomerization.

Complex, natural product derived substrates can also be silylated using this protocol. For example, silylation of an allylated cholesterol derivative gave rise to allylsilane **25** in excellent yield. Importantly, this example also demonstrates that terminal alkenes are silylated selectively over internal alkenes, and that stereogenic centers at the homoallylic position of the starting material can be maintained with full stereochemical fidelity during the reaction.

The effect of steric bulk proximal to the site of  $\beta$ -hydride-elimination was studied by the preparation of allylsilanes **26**–**28**. In particular, we desired to understand the effects of steric crowding on allyl- vs vinylsilane selectivity. With modest levels of steric encumbrance (tertiary carbon center) at either the  $\delta$ - or  $\epsilon$ -position relative to the terminal alkene starting material, no erosion of selectivity for allylsilanes was observed (**26** and **27**). In fact, even branching at the  $\delta$ -position resulted in good selectivity for allylsilanes as long as there was a hydrogen atom available for  $\beta$ -hydride-elimination (**28**). Notably, however, in these more sterically encumbered cases, a slight increase in catalyst loading was required to maintain high yield (see Figure 3). We attribute this requirement to increased difficulty in the migratory insertion step.

In contrast, more severe steric interactions did decrease selectivity for allylsilanes. For example, the presence of a fully substituted carbon at the  $\gamma$ -position of the starting material noticeably decreased selectivity, leading to a 72:28 mixture of allyl and vinyl isomers (**29**, see Discussion below). Interestingly, however, when trimethylallylsilane was used, the product symmetry allows for the production of unsaturated disilane **30** as a single isomer.

With our previous catalyst system, we observed poor allyl vs vinyl selectivity in the formation of silyl ether **31**. As we believed this to be an informative reaction in understanding the factors controlling allyl vs vinyl selectivity, we reinvestigated this reaction using the second-generation catalyst (Figure 3). While the yield of **31** is greatly improved using the new catalyst, a similar mixture of isomeric products is observed. The reasons for this erosion of selectivity are discussed below.

Finally, in our previous study, aryl-substituted allyl compounds were a particularly challenging class of substrates due to the propensity of the alkene of the starting material to migrate into conjugation with the aromatic group. Second-generation ligand **14** provides vastly improved silyl-Heck reactions across a range of such substrates (**32**–**37**, Figure 4). With electron-neutral and heteroaromatic substrates, very little alkene isomerization was observed (**33** and **37**). With highly electron-rich allyl aromatic substrates, alkene isomerization could not be fully suppressed, resulting in slightly diminished yields (**32**, **34**–**36**). However, in all cases, reactions involving ligand **14** were dramatically improved over those using <sup>t</sup>BuPPh<sub>2</sub>. In these cases, only the *E*-allylsilanes are observed. In no case, were *Z*-allyl- or vinylsilane was detected (NMR and GC/MS).

**2.5. Steric and Electronic Effects in Allylsilane vs Vinylsilane Selectivity.** As mentioned above, the limited amount of alkene isomerization observed in the formation of compounds **23** and **24** suggests that the observed allyl/vinyl ratio is likely kinetic in nature. To further determine if the allylsilane products might arise from isomerization of vinylsilanes under the reaction conditions, we independently prepared vinylsilane **38** and added it to the silyl-Heck reaction of 1-hexene and Me<sub>3</sub>SiI (Scheme 1). After the reaction, allylsilane

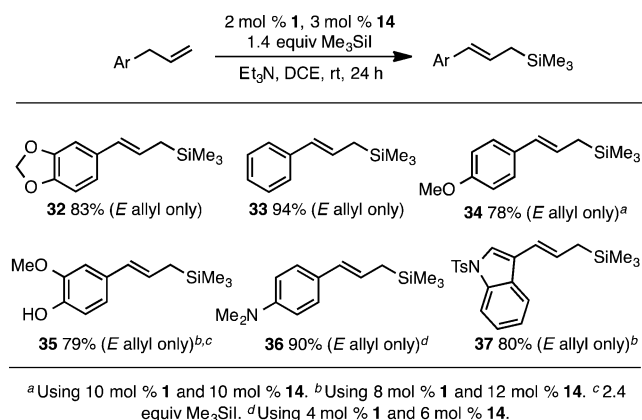
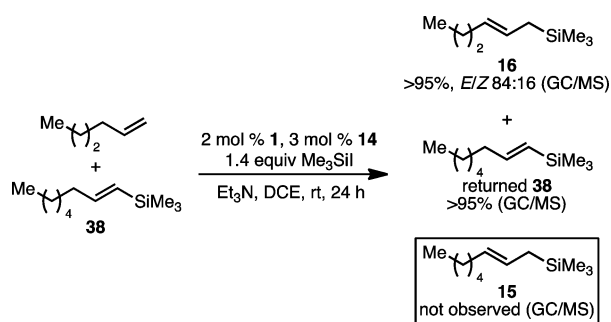


**Figure 4.** Silyl-Heck reactions with aryl-substituted allyl substrates.

### Scheme 1. Kinetic Stability of Vinylsilanes Under Silyl-Heck Reaction Conditions



**16** (arising from 1-hexene) was observed in quantitative yield (>95%, GC/MS). In addition, vinylsilane **38** remained unchanged, being returned from the reaction in >95% yield (GC/MS). Importantly, allylsilane **15**, which is the product of alkene isomerization of **38**, was not detected. These results support the proposal that the observed allyl/vinyl ratios from the silyl-Heck reaction are kinetic in nature, and implicates  $\beta$ -hydride elimination from the alkyl-palladium intermediate as the product-determining step.

Allylsilanes are typically the vastly major product in this class of silyl-Heck reactions. These products result from  $\beta$ -hydride elimination away from the silicon center, and in principle either steric or electronic factors could contribute to the observed selectivity. The observed ratio of allyl- and vinylsilanes in the formation of *tert*-butyl substituted product **29** (Figure 3) sheds considerable light on the nature of this selectivity.

Considering allyl-palladium intermediate **38** that forms en route to **29**,  $\beta$ -hydride elimination can occur either toward the *tert*-butyl group or the trimethylsilyl group in an otherwise symmetrical molecule (Figure 5). As the *tert*-butyl group

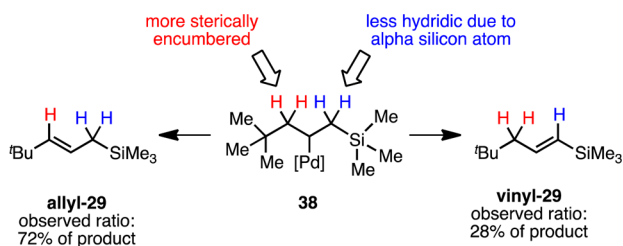


**Figure 5.** Steric vs Electronic Control in  $\beta$ -Hydride Elimination Leading to Product **29**.

(*A*-value = 4.9 kcal/mol) is larger than the trimethylsilyl group (*A*-value = 2.5 kcal/mol), strictly steric selectivity would favor formation of vinylsilane product vinyl-**29**.<sup>9</sup> In contrast, due to the  $\alpha$  silicon effect and the fact that the hydrogen atoms  $\alpha$  to the silicon center have increased acidity and decreased hydricity,<sup>10</sup> electronic control would favor  $\beta$ -elimination toward the *tert*-butyl group. The fact that allylsilane allyl-**29** is the dominant product suggests a significant electronic contribution in product determination in the silyl-Heck reaction. The importance of electronic factors in  $\beta$ -hydride elimination have been documented in other palladium-catalyzed Heck-type reactions.<sup>11,12</sup>

Importantly, in substrates lacking such bulk substituents, such as those leading to allylsilanes **2** and **15–28**, the large trimethylsilyl group is the most sterically demanding in the proximity of the palladium center in the metal alkyl intermediate. In such cases, steric and electronic factors reinforce each other, helping to explain the high allylsilane selectivity observed.

Finally, we believe electronic factors also explain the low allyl/vinyl ratio observed in the formation of product **31** (Figure 3). Product **27** provides a comparable steric environment to this product. However, unlike **31**, the formation of compound **27** vastly favors formation of the allyl isomer, ruling out steric factors as an explanation for the observed selectivity in **31**. Instead, we believe that the poor selectivity observed in the formation of **31** is primarily electronic in nature and is due to the lowered hydricity of the hydrogen atoms  $\beta$  to the electron-withdrawing ether and aromatic group.

This deeper understanding of the importance of electronic, as well as steric, factors in product selection will undoubtedly be important in planning synthetic applications of the silyl-Heck reaction in complex allylsilane synthesis.

### 2.6. Understanding the Effects of Steric and Electronic Ligand Properties on the Silyl-Heck Reaction.

Having demonstrated that ligand **14** is vastly superior to the earlier system in the formation of allylsilanes, we wanted to better understand how the electronic and steric properties of the various ligands contributed to their performance in the silyl-Heck reaction.

To gauge the steric properties of the ligands, we obtained X-ray crystal structures of the ligands that could be crystallized (in all, 8 of the 12 ligands studied). Using these structures, we computed the Equivalent Cone Angle (ECA), employing the method of Guzei and assuming a metal-phosphine bond distance of 2.28 Å (Table 2).<sup>13,14</sup>

From these data, and in comparison to the data presented in Table 1, the importance of size becomes obvious. In general, ligands with larger steric size outperform smaller ligands. Further, the best performing ligands (**8**, **11**, and **14**) have the largest computed cone angles.<sup>15</sup>

Steric data, however, do not provide a complete explanation for the variance in ligand performance. In particular, these data do not explain the superiority of ligands **11** and **14** (ECA 149° for both) over ligand **8** (ECA 153°). In particular, ligands **8** and **14** differ only by the presence of a *para*-methoxy group on the aromatic rings. The difference in the ECAs appears to be too small (and is in opposite trend) to explain the difference in reactivity.

To gauge the  $\sigma$ -donor ability of the ligands, each was converted to the phosphine selenide by treatment with elemental (black) selenium in CDCl<sub>3</sub>. Previous studies have shown that the  $\sigma$ -donor ability of phosphine ligands is directly proportional to the inverse of the <sup>31</sup>P–<sup>77</sup>Se coupling constant in the NMR spectra (<sup>1</sup>J<sub>P–Se</sub>).<sup>16,17</sup> Measurement of this coupling constant for

Table 2. Computed Equivalent Cone Angles (ECA) of Ligands

Entry	Ligand	Ar	R	ECA <sup>a</sup>
1	3	R	H	134°
2	4		OMe	–
3	5		CF <sub>3</sub>	–
4	6	R	H	–
5	7		Me	138°
6	8		<sup>t</sup> Bu	153°
7	9	R	H	135°
8	10		Me	134°
9	11		<sup>i</sup> Pr	149°
10	12	R	Me	133°
11	13		<sup>i</sup> Pr	–
12	14		<sup>t</sup> Bu	149°

<sup>a</sup>ECA = Equivalent Cone Angle, M–P bond = 2.28 Å.Table 3. <sup>31</sup>P–<sup>77</sup>Se Coupling Constants of Phosphine Selenides

Entry	Ligand	Ar	R	<sup>1</sup> J <sub>P–Se</sub> <sup>a</sup>
1	3	R	H	716
2	4		OMe	720
3	5		CF <sub>3</sub>	766
4	6	R	H	707
5	7		Me	704
6	8		<sup>t</sup> Bu	705
7	9	R	H	688
8	10		Me	698
9	11		<sup>i</sup> Pr	696
10	12	R	Me	707
11	13		<sup>i</sup> Pr	707
12	14		<sup>t</sup> Bu	698

<sup>a</sup><sup>1</sup>J<sub>P–Se</sub> measured in CDCl<sub>3</sub> from in situ generated phosphine selenide.

each of the in situ generated phosphine selenides revealed three trends (Table 3).<sup>18</sup> First, as expected, the substituted ligands bearing electron-donor groups are in fact more electron-rich than the parent <sup>t</sup>BuPPh<sub>2</sub>. Second, while electron-rich ligands give generally improved catalytic performance, only those ligands that are also sterically bulky provide highly improved results compared to <sup>t</sup>BuPPh<sub>2</sub>. For example, ligand 9 bearing the *N,N*-dimethylaniline group is measured to be the most electron-rich, but its small cone angle and exposed basic amine make it only negligibly better than <sup>t</sup>BuPPh<sub>2</sub>. Third, 11 and 14 are two of the most electron-rich ligands and appear to have greater  $\sigma$ -donor ability than ligand 8.

In the context of the silyl-Heck reaction, the ligand data outlined above correlate very strongly with the observed trends in yield. The two most effective ligands (11 and 14) are the two with the best combination of electron-richness and large steric size. These factors are expected to favor oxidative addition, and are consistent with our hypothesis that led to the rational design of these second-generation ligands.

A more subtle result that emerges from the electronic analysis of the ligands is the comparative lack of electron-richness of ligand 8, particularly compared to ligand 14, which lacks the presumably electron-donating *para*-methoxy group. One possible explanation for this surprising result is that the large flanking alkyl groups of ligand 8 restrict the conformation of the methoxy group to be out of plane with the aromatic ring, so that the beneficial overlap between the nonbonding electrons on the oxygen and the  $\pi$ -system of aromatic ring is poor and offset by the inductive electron-withdrawing effect of the oxygen atom.

We believe that this is the first time that the electronic properties of these large phosphine substituents have been quantified in a systematic way. Beyond the scope of the silyl-Heck reaction, these data might inform on ligand design in other classes of novel sterically demanding, electron-rich phosphine ligands.

**2.7. Insights into Catalyst Structure.** The silyl-Heck reactions with this second-generation ligand (as well as with the other high-yielding ligands presented herein) are particularly sensitive to the ligand/metal (L/M) ratio employed. Empirically (as reflected in Figure 2), L/M ratios between 1:1 and 1.5:1 provide the highest yields of allylsilanes. With L/M ratios at or above 2:1, a pronounced drop in reactivity is observed. These results are suggestive of the importance of low-valent metal centers in the catalytic reaction.<sup>19</sup>

To further probe the relevance of low-valent palladium complexes in silyl-Heck reactions using our second-generation ligands, stoichiometric experiments were undertaken. These studies shed considerable light onto the catalytic process. For example, combining ligand 7 with precatalyst 1 and excess Me<sub>3</sub>SiI in a solvent mixture of toluene, benzene, and pentane at –35 °C results in the formation of light green crystals, which were determined to be oxidative addition complex 39 using X-ray crystallography (Figure 6). This thermally and air-sensitive

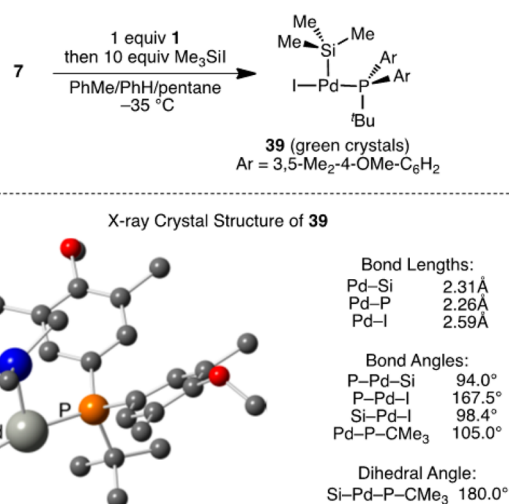


Figure 6. Preparation and structure of complex 39.

T-shaped monophosphine complex has an open coordination site opposite the silicon ligand (no intramolecular interactions, including agostic interactions with the *tert*-butyl group, nor intermolecular interactions are observed in this open coordination site). This compound is the first monomeric palladium complex resulting from oxidative addition of a silicon–halide bond to be characterized, and is also the first such complex to be supported by a phosphine ancillary ligand.<sup>20</sup> This complex was fully characterized in solution (<sup>1</sup>H, <sup>13</sup>C and <sup>31</sup>P NMR in CD<sub>2</sub>Cl<sub>2</sub> at 0 °C), and the data are consistent with the structure shown in Figure 6.

Complex **39** is a competent precatalyst in the silyl-Heck reaction. The use of 2 mol % of this complex with an additional 1 mol % of **7** as catalyst (mimicking the optimized metal/ligand ratio) provided allylsilane **2** in 72% yield, which is comparable to the in situ generated catalyst (Table 1). Further, complex **39** is the major product observed (<sup>31</sup>P NMR) in stoichiometric experiments performed in DCE (1 equiv each of **1** and **7**, 15 equiv each of Me<sub>3</sub>SiI and Et<sub>3</sub>N), which is the solvent of choice for the catalytic reaction. Combined, these experiments establish the relevance of complex **39** under catalytically relevant conditions. Finally and significantly, a highly similar signal is observed by <sup>31</sup>P NMR when ligand **14** is used in the stoichiometric reaction (in DCE, as above), suggesting that an analogous complex is formed with the optimal ligand.<sup>21</sup> To date, however, we have been unable to crystallize the complex using the more soluble ligand **14**.

These results, along with the steric and electronic data outlined above and the optimized reaction conditions, are highly suggestive that the active catalyst is a palladium–monophosphine (L<sub>1</sub>M) complex. Such a catalytic intermediate parallels those involved in oxidative additions of carbon–halogen bonds using large, electron-rich phosphines.<sup>7</sup> Moreover, the structure of **39**, particularly the disposition of the aromatic groups on the phosphine, clearly illustrates how this class of diaryl-*tert*-butylphosphine ligands accommodates the steric bulk of the large Me<sub>3</sub>Si group. The rotation of these groups away from the silicon center is consistent with our previous hypothesis for why these ligands are superior in the silyl-Heck reaction.<sup>2</sup>

### 3. CONCLUSIONS

Using rational ligand design, we have developed an easily prepared, bench-stable second-generation ligand for the preparation of allylsilanes using the silyl-Heck reaction. Unlike the previously reported system, the new ligand provides extremely high yields of allylsilane products using simple terminal  $\alpha$ -olefin substrates, with good *E/Z* selectivity, very little formation of vinylsilanes, and only trace isomerization of the alkene starting materials. Quantitative studies demonstrate that this new ligand is much larger and more electron-rich than the first-generation ligand, and the isolation of an oxidative addition complex of Me<sub>3</sub>SiI sheds significant light onto the effectiveness of this ligand class. Overall, we believe that this new ligand provides a simple, direct, and highly useful means to access high-value allylsilanes from readily available starting materials using the silyl-Heck reaction.

### ■ ASSOCIATED CONTENT

#### Supporting Information

Experimental procedures, crystallographic, and spectral data. This material is available free of charge via the Internet at <http://pubs.acs.org>

### ■ AUTHOR INFORMATION

#### Corresponding Author

dawatson@udel.edu

#### Notes

The authors declare no competing financial interest.

### ■ ACKNOWLEDGMENTS

Mr. Gabriel Andrade (UD) is thanked for assistance with crystallography. The University of Delaware (UD), the Research Corporation (Cottrell Scholars Program), and the NSF (CAREER CHE1254360) are gratefully acknowledged for support. NMR and other data were acquired at UD on instruments obtained with the assistance of NSF and NIH funding (NSF CHE0421224, CHE1229234, CHE0840401, and CHE1048367; NIH P20 GM103541 and S10 RR02692).

### ■ REFERENCES

- (1) (a) Brook, M. A. *Silicon in Organic, Organometallic, and Polymer Chemistry*; Wiley: Chichester, 2000. (b) Fleming, I., *Organic Silicon Chemistry*. In *Comprehensive Organic Chemistry*; Barton, D. H. R., Ollis, W. D., Eds.; Pergamon: Oxford, 1979; Vol. 3, p 539. (c) Fleming, I. *Allylsilanes, Allylstannanes, and Related Systems*. In *Comprehensive Organic Synthesis*; Trost, B. M., Fleming, I., Eds.; Pergamon: Oxford, 1991; Vol. 2, p 563. (d) Fleming, I.; Dunoguès, J.; Smithers, R. The Electrophilic Substitution of Allylsilanes and Vinylsilanes. In *Organic Reactions*; John Wiley & Sons, Inc.: New York, 2004; p 57. (e) Sarkar, T. K., Allylsilanes. In *Science of Synthesis*; Fleming, I., Ed.; Thieme: Stuttgart, 2001; Vol. 4, p 837. (f) Hosomi, A. *Acc. Chem. Res.* **1988**, *21*, 200. (g) Yamamoto, Y.; Asao, N. *Chem. Rev.* **1993**, *93*, 2207. (h) Masse, C. E.; Panek, J. S. *Chem. Rev.* **1995**, *95*, 1293. (i) Denmark, S. E.; Fu, J. *Chem. Rev.* **2003**, *103*, 2763. (j) Fleming, I.; Barbero, A.; Walter, D. *Chem. Rev.* **1997**, *97*, 2063.
- (2) McAtee, J. R.; Martin, S. E. S.; Ahneman, D. T.; Johnson, K. A.; Watson, D. A. *Angew. Chem., Int. Ed.* **2012**, *51*, 3663.
- (3) For other silyl-Heck reactions, see: (a) Martin, S. E. S.; Watson, D. A. *J. Am. Chem. Soc.* **2013**, *135*, 13330. (b) McAtee, J. R.; Martin, S. E. S.; Cinderella, A. P.; Reid, W. B.; Johnson, K. A.; Watson, D. A. *Tetrahedron* **2014**, *70*, 4250.
- (4) For a review of the development of the silyl-Heck reaction, see: Martin, S. E. S.; Watson, D. A. *Synlett.* **2013**, *24*, 2177.
- (5) For early work in the silyl-Heck area, see: (a) Yamashita, H.; Kobayashi, T.; Hayashi, T.; Tanaka, M. *Chem. Lett.* **1991**, *20*, 761. (b) Chatani, N.; Amishiro, N.; Murai, S. *J. Am. Chem. Soc.* **1991**, *113*, 7778. (c) Chatani, N.; Amishiro, N.; Morii, T.; Yamashita, T.; Murai, S. *J. Org. Chem.* **1995**, *60*, 1834. (d) Terao, J.; Torii, K.; Saito, K.; Kambe, N.; Baba, A.; Sonoda, N. *Angew. Chem., Int. Ed.* **1998**, *37*, 2653. (e) Terao, J.; Jin, Y.; Torii, K.; Kambe, N. *Tetrahedron* **2004**, *60*, 1301.
- (6) For a related transformation, see: Nakamura, S.; Yonehara, M.; Uchiyama, M. *Chem.—Eur. J.* **2008**, *14*, 1068.
- (7) (a) Christmann, U.; Vilar, R. *Angew. Chem., Int. Ed.* **2005**, *44*, 366. (b) Corbet, J.-P.; Mignani, G. *Chem. Rev.* **2006**, *106*, 2651. (c) Hartwig, J. F. *Synlett* **2006**, *2006*, 1283. (d) Fu, G. C. *Acc. Chem. Res.* **2008**, *41*, 1555. (e) Fleckenstein, C. A.; Plenio, H. *Chem. Soc. Rev.* **2010**, *39*, 694. (f) Surry, D. S.; Buchwald, S. L. *Chem. Sci.* **2011**, *2*, 27.
- (8) See SI for exact allyl/vinyl selectivity.
- (9) (a) Winstein, S.; Holness, N. J. *J. Am. Chem. Soc.* **1955**, *77*, 5562. (b) Kitching, W.; Olszowy, H. A.; Drew, G. M.; Adcock, W. J. *Org. Chem.* **1982**, *47*, 5153.
- (10) (a) Whitmore, F. C.; Sommer, L. H. *J. Am. Chem. Soc.* **1946**, *68*, 481. (b) Colvin, E. W. *Silicon in Organic Synthesis*; Butterworths: London, 1981. (c) Takahashi, O.; Morihashi, K.; Kikuchi, O. *Bull. Chem. Soc. Jpn.* **1991**, *64*, 1178. (d) Brinkman, E. A.; Berger, S.; Brauman, J. I. *J. Am. Chem. Soc.* **1994**, *116*, 8304.
- (11) Werner, E. W.; Sigman, M. S. *J. Am. Chem. Soc.* **2011**, *133*, 9692.
- (12) Recently, iridium-catalyzed dehydrogenative silylation of alkenes to form vinylsilanes have been reported.  $\beta$ -hydride elimination from a

$\beta$ -silyl alkyl metal hydride complex has been proposed as a key step in those processes. However, it appears to occur towards the silicon center in those cases. See: (a) Cheng, C.; Simmons, E. M.; Hartwig, J. F. *Angew. Chem., Int. Ed.* **2013**, *52*, 8984. (b) Lu, B.; Falck, J. J. *Org. Chem.* **2010**, *75*, 1701.

(13) Guzei, I. A.; Wendt, M. *Dalton Trans.* **2006**, 3991.

(14) Tolman, C. A. *Chem. Rev.* **1977**, *77*, 313.

(15) The larger than expected cone angle of ligand **11**, which contains meta isopropyl substituents on the aromatic rings, is explained by the gearing of those groups off of the adjacent *para*-dimethylamino groups. This conformation, which is observed in the X-ray crystal structure, makes the isopropyl groups project steric bulk similar to *tert*-butyl groups. See CIF in SI for further details.

(16) (a) Pinnell, R. P.; Megerle, C. A.; Manatt, S. L.; Kroon, P. A. *J. Am. Chem. Soc.* **1973**, *95*, 977. (b) Allen, D. W.; Taylor, B. F. *J. Chem. Soc., Dalton Trans.* **1982**, 51. (c) Socol, S. M.; Verkade, J. G. *Inorg. Chem.* **1984**, *23*, 3487. (d) Socol, S. M.; Verkade, J. G. *Inorg. Chem.* **1986**, *25*, 2658. (e) Beckmann, U.; Süslüyan, D.; Kunz, P. C. *Phosphorus, Sulfur Silicon Relat. Elem.* **2011**, *186*, 2061.

(17) For recent applications of this method, see: (a) Sergeev, A. G.; Spannenberg, A.; Beller, M. *J. Am. Chem. Soc.* **2008**, *130*, 15549. (b) Berhal, F.; Esseiva, O.; Martin, C.-H.; Tone, H.; Genet, J.-P.; Ayad, T.; Ratovelomanana-Vidal, V. *Org. Lett.* **2011**, *13*, 2806. (c) Kawaguchi, S.-i.; Minamida, Y.; Ohe, T.; Nomoto, A.; Sonoda, M.; Ogawa, A. *Angew. Chem., Int. Ed.* **2013**, *52*, 1748.

(18) It is known that  $^1J_{P,Se}$  is sensitive to the pyramidalization of the phosphine atom, which can be affected by steric bulk of the phosphorus substituents. See ref 16e. However, analysis of the X-ray crystal structures reveals that the pyramidalization is nearly identical in all ligands studied (see SI for details). Thus, we believe the differences in coupling constants for the phosphine selenides reflects electronic differences at the phosphorus center.

(19) Littke, A. F.; Dai, C.; Fu, G. C. *J. Am. Chem. Soc.* **2000**, *122*, 4020.

(20) Esposito, O.; Roberts, D. E.; Cloke, F. G. N.; Caddick, S.; Green, J. C.; Hazari, N.; Hitchcock, P. B. *Eur. J. Inorg. Chem.* **2009**, 2009, 1844.

(21) See SI for details.